Adaptive neural dynamic surface control for nonstrict-feedback systems with output dead-zone

Xiaocheng Shi, Cheng-Chew Lim, Senior Member, IEEE, Peng Shi, Fellow, IEEE, and Shengyuan Xu

***Abstract*—This paper focuses on the problem of adaptive output-constrained neural tracking control for uncertain nonstrict-feedback systems in the presence of unknown symmetric output dead-zone and input saturation. A Nussbaum-type function-based dead-zone model is introduced such that the dynamic surface control approach can be used for controller design. The variable separation technique is employed to decompose the unknown function of entire states in each subsystem into a series of smooth functions. Radial basis function neural networks are utilized to approximate the unknown black-box functions derived from Young's inequality. With the help of auxiliary first-order filters, the dimensions of neural network input are reduced in each recursive design. A main advantage of the proposed method is that for an n-order nonlinear system, only one adaptation parameter needs to be tuned online. It is rigorously shown that the proposed output-constrained controller guarantees that all the closed-loop signals are semi-global uniformly ultimately bounded and the tracking error never violates the output constraint.**

***Index Terms*—Dynamic surface control; Neural networks; Output dead-zone; Nonstrict-feedback nonlinear systems; Adaptive output-constrained control.**

I. Introduction

CONTROL of nonstrict-feedback nonlinear systems has become an active topic recently because nonstrict-feedback structure has a more general and complete form than strict-feedback model in system dynamics, which can be used to construct physical systems, such as the helicopter model [1], the ball-and-beam control system [2], and nonlinear oscillatory model of chemical process [3]. Meanwhile, neural networks (NNs) or fuzzy logic systems (FLSs) [4], [5] as universal approximators combined with adaptive backstepping control technique have been extensively studied for controlling uncertain strict-feedback nonlinear systems [6]−[18], but the technique cannot be directly applied to nonstrict-feedback nonlinear systems. The difficulty comes from the problem of circular construction of controller due to each subsystem function containing the whole states. In addition, meeting practical constraints may degrade the control system performance. To date, specific consideration of tracking error constraints under the nonstrict-feedback structure has received little attention.

Driven by both practical demands and theoretical challenges, in [19], [20], two rigorously derived adaptive tracking control schemes using backstepping control were given for nonstrict-feedback nonlinear systems. Furthermore, by designing an appropriate Lyapunov-Krasovskii functional, time-delay of plants with uncertain stochastic signals were considered in developing approximation-based adaptive fuzzy control method in [3]. The aforementioned adaptive neural/fuzzy controller design in [3], [19], [20] is feasible under the condition that the state variables are measurable, to relax such restriction, a new output-feedback adaptive neural approach was proposed for a class of nonstrict-feedback systems with unmeasurable state variables by fusing backstepping design with the observer technique in [21]. By estimating the norm of the fuzzy/neural weight vector, the number of on-line tuning parameters significantly decreased to n for an n-order systems in [3], [19]−[21]. This method was further improved in [18] with the purpose of allowing for general design with stability, where only one learning parameter needed to be updated. It was found that above nonstrict-feedback systems design methods in [3], [19]−[22] suffer from the problem of intricate controller design, which is mainly caused by repeatedly differentiating some nonlinear functions.

On the other hand, to solve the "explosion of terms" problem, a dynamic surface control (DSC) technique was first proposed in [23] for strict-feedback systems, in which a first-order filter is introduced at each step of the backstepping design procedure. Subsequently, adaptive DSC approach was proposed to address a NN-based tracking problem for a class of uncertain strict-feedback nonlinear systems in [24] and the perturbed pure-feedback nonlinear systems in [25]. In [26], adaptive DSC design was studied for multi-agent systems where a direct graph-based error surface was proposed to achieve the distributed consensus tracking performance. In [27], based on the approximation property of radial basis function neural networks (RBFNNs), a Nussbaum type function was employed to deal with the unknown direction control gains by integrating the DSC with Lyapunov synthesis theory. Adaptive fuzzy DSC design was first examined to address the output-constrained problem in conjunction with the Barrier Lyapunov Function (BLF) in [28]. Furthermore, in [29], an observer-based adaptive output-feedback scheme was proposed for a class of partial tracking error constrained MIMO nonlinear systems by introducing predefined performance with DSC. Despite these efforts, to the best of our knowledge, there are no other results for approximation-based adaptive tracking problem of nonlinear systems with nonstrict-feedback framework using DSC technique.

Dead-zone as one of the nonsmooth nonlinearities often found in physical systems, such as electronic relay circuits, hydraulic servo-valve, and biology optics. Their existence

X. Shi, and S. Xu are with the School of Automation, Nanjing University of Science and Technology, Nanjing 210094, China (email: nihaoshixiaocheng@gmail.com; syxu@njust.edu.cn).

C. Lim, and P. Shi are with the School of Electrical and Electronic Engineering, The University of Adelaide, Adelaide, S.A. 5005, Australia (e-mail: cheng.lim@adelaide.edu.au; Peng.Shi@adelaide.edu.au).

severely degrades the system performance, and makes the control system oscillatory or even unstable. Numerous studies [13], [16], [17], [25], [30]−[35] on controlling nonlinear systems with input dead-zone were made using adaptive control techniques. In [33], by using a sum of squares optimization algorithm and rewriting the dead-zone as a bounded disturbance, an adaptive output feedback control stabilization problem was studied for a class of uncertain nonlinear systems with an unknown dead-zone nonlinearity without constructing the dead-zone inverse. A similar way of dead-zone compensation was used to solve the exact tracking control problem for a class of nonlinear systems with time delays and dead-zone input in [34]. However, the bounds of the slopes and the breakpoint of dead-zone are required to be known in [33], [34]. To relax such a restriction, based on NNs approximation, an adaptive backstepping control scheme was proposed for a class of switched stochastic nonlinear systems with actuator dead-zone in [35]. While the effects of dead-zone in the actuator is important, practical systems may also suffer from the output dead-zone nonlinearity. However, they receives relatively little attention until recently, an adaptive fuzzy tracking problem was studied in [36], which focused on strict-feedback systems with dead-zone output mechanism based on adaptive fuzzy backstepping technique. If the nonlinear systems appeared in nonstrict-feedback form are subject to unknown symmetric output dead-zone and are required to be stabilized by adaptive neural DSC-based controller, to the best of our knowledge, there are no such existing schemes, furthermore, when output tracking error cannot exceed the prescribed constraints, the control design becomes more complicated.

The motivation of this study is two-fold. First, nonstrict-feedback nonlinear systems can model many autonomous control systems. When not taking into account in the control design stage non-smooth nonlinearities such as output dead-zone and input saturation, it will degrade the system performance, which should be explicitly considered for the stability and improved system behaviour. When taking into account performance limits and/or safety requirements in practice, tracking error constraints must be considered. Second, abbreviating learning time has always been an important topic in adaptive neural network control. Hence, this paper investigates the problem of adaptive output-constrained tracking control to achieve efficient tracking and computational performance for nonstrict-feedback nonlinear systems with symmetric output dead-zone and input saturation. The BLF is used for preventing the violation of error output constraints. Approximation-based adaptive DSC is employed to design the adaptive neural control, which alleviates the complexity of the controller design procedure and the burdensome computation as the order of the nonlinear system increases but is not directly applicable to more general nonlinear systems. Therefore, more general adaptive DSC control scheme based on variable separation technique will be extended in this paper to facilitate control design of nonstrict-feedback systems with unknown symmetric output dead-zone and input saturation.

The main contributions from this paper are as follows.

(1) A novel DSC-based adaptive neural control is proposed for a class of nonstrict-feedback systems to handle both error output constraints and unknown symmetric output dead-zone. The explosion of complexity caused by repeatedly differentiating some nonlinear functions in [3], [19]−[22] is overcome by using auxiliary first-order filters. In addition, the dimensionality explosion of neural network input vector caused by approximating nonlinear functions is overcome by using the derivative of the filter output as the NNs input.

(2) Effective methods to tune adaptation parameters are proposed in [3], [7], [8], [16], [17], [19]−[21], [31], [36] by using the norms of the NNs/FLSs weights. However, in our work, only one on-line estimation parameter needs to be updated for an n-order nonlinear nonstrict-feedback system. It is therefore more efficient and useful.

(3) Compared with the existing results of tracking problem in [3], [8], [9], [13], [14], [17], [20], [34], [36]−[38] the control method in this paper only requires the known information of the desired trajectory and its first time derivative. Thus, the assumption on desired trajectory imposed in our paper is more reasonable for practical applications.

The rest of this paper is organized as follows. In Section II, we explain the problem formulation and mathematical preliminaries. The adaptive DSC design procedure and the analysis of stability are presented in Section III. Three simulations are performed to illustrate the effectiveness of the proposed approach in Section IV. Some conclusions are summarized in Section V.

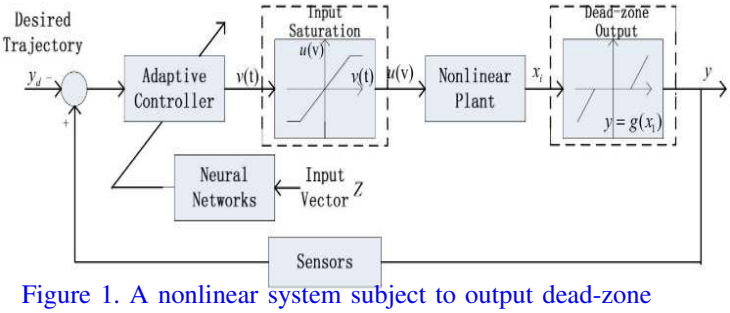

Figure 1. A nonlinear system subject to output dead-zone and input saturation

II. Problem Formulation and Preliminaries

Consider the following uncertain nonlinear dyanmic system in nonstrict-feedback form with the unknown dead-zone output and input saturation:

$$\begin{cases} \dot{x}_i = x_{i+1} + f_i(x) + d_i(x,t), i = 1, ..., n-1 \\ \dot{x}_n = u(v) + f_n(x) + d_n(x,t) \\ y = g(x_1) \end{cases} \tag{1}$$

where $x = [x_1, \ldots, x_n]^{\mathrm{T}} \in R^n$ represents the state vector with $\bar{x}_i = [x_1, \ldots, x_i]^{\mathrm{T}} \in R^i$, $v(t) \in R$ is the input of controller and $u(v)$ represents the system input, $y \in R$ denotes the system output, and $d_i(x,t)(i = 1, \ldots, n) : R^n \times R \to R$ are bounded disturbances due to measurement noise or sensor noise [41]. The function $f_i(x)(i = 1, \ldots, n) : R^n \to R$ are unknown smooth functions of all states with $f_i(0) = 0$, and $g(x_1)$ is the symmetric dead-zone nonlinearity. The dead-zone nonlinearity is characterized as follows:

$$y = g(x_1) = \begin{cases} m(x_1 - b), x_1 > b \\ 0, -b \le x_1 \le b \\ m(x_1 + b), x_1 < -b \end{cases} \tag{2}$$

where $m > 0$ stands for the slope of the dead-zone, and $b > 0$ denotes the dead-zone width parameter. The symmetric dead-zone output takes the form as shown in Fig. 2. The saturation nonlinearity $u(v)$ is represented as [39]:

$$u(v(t)) = \text{sat}(v(t)) = \begin{cases} \text{sign}(v(t))u_s, |v(t)| \geq u_s \\ v(t), |v(t)| < u_s \end{cases}$$

where u_s is the bound of $u(v(t))$. We observe that $u(v(t))$ is non-differentiable at the sharp corner $|v(t)| = u_s$. Hence, we use a smooth model to approximate the saturation nonlinearity as follows:

$$p(v(t)) = u_s \tanh(\frac{v(t)}{u_s}) = u_s \frac{e^{v(t)/u_s} - e^{-v(t)/u_s}}{e^{v(t)/u_s} + e^{-v(t)/u_s}}$$

Then $\text{sat}(v(t))$ changes to

$$\text{sat}(v(t)) = p(v(t)) + \Delta(v(t)) = u_s \tanh(\frac{v}{u_s}) + \Delta(v(t)) \quad (3)$$

where $\Delta(v) = \text{sat}(v(t)) - p(v(t))$ is the difference between the saturation model and the approximation model. Then, we have the bound of $\Delta(v)$ as

$$|\Delta(v(t))| = |\text{sat}(v(t)) - p(v(t))| \leq u_s(1 - \tanh(1)) = \bar{d}$$

To facilitate the DSC design later, according to the mean-value theorem [40], the smooth function $p(v(t))$ can be expressed as

$$p(v(t)) = p(v^0) + p_{v^\mu}(v - v^0)$$

where $p_{v^\mu} = \frac{\partial p(v(t))}{\partial v}\Big|_{v=v^\mu}$ and $v^\mu = \mu v + (1-\mu)v^0$ with $0 < \mu < 1$. Considering $v^0 = 0$, we obtain

$$p(v(t)) = p_{v^\mu} v(t)$$

The control objective is to design an adaptive neural controller v such that the system output $y(t)$ tracks a desired reference signal y_d while ensuring all the closed-loop signals remain semi-global uniformly ultimately bounded (SGUUB), and that the tracking error constraint $|s_1(t)| = |y(t) - y_d| \leq k_{b1}$ is met, where k_{b1} is a positive prescribed constant. Fig. 1 shows the block diagram of the nonlinear control system under the adaptive neural control to be presented in the sections that follow.

To proceed, we introduce the following assumptions on system (1).

Assumption 1: The desired trajectory y_d and its first derivative $\dot{y}_d$ are available. It is further assumed that there exists an unknown positive constant d^* such that $|y_d| \leq d^*$.

Assumption 2: There exist unknown strictly increasing smooth functions $\phi_i(\cdot)$ with $\phi_i(0) = 0$ such that $|f_i(x)| \leq \phi_i(\| x \|), i = 1, \cdots, n$.

Assumption 3: For the continuous functions $d_i(x,t) : R^n \times R \to R, i = 1, \ldots, n$, there exist unknown continuous functions $\chi_i(\bar{x}_i)$ and positive constants p_i^* such that $|d_i(x,t)| \leq \chi_i(\bar{x}_i)p_i^*$.

To describe Assumption 4, we introduce the following change of coordinates based on the dynamic surface control technique:

$$s_1 = y(t) - y_d \quad (4)$$

$$s_k = x_k - z_k \quad (5)$$

$$y_k = z_k - \alpha_k \quad (6)$$

where $k = 2, \ldots, n$, s_k is the error surface, z_k is the output of the first-order filter, y_k is the boundary layer error, and α_k is the virtual control signal, which will be specified later.

Assumption 4: For the continuous function α_2, there exists a positive constant ρ_1 such that the inequality $|\alpha_2| \leq \rho_1|s_1|$ is satisfied.

Assumption 5: For the function p_{v^μ}, there exists a positive constant g_m such that $0 < g_m < p_{v^\mu} < 1$.

Remark 1: Notice that Assumption 1 gives a milder restriction condition on the desired trajectory compared with the tracking control results in [3], [7], [8], [16], [17], [19]–[21], [31], [36]. Assumption 2 is commonly used in [3], [19]–[22] when dealing with the control problem for nonlinear systems in nonstrict-feedback form. Assumption 3 indicates that external disturbances have finite energy and, hence, are bounded [41], [42]. Assumption 4 is similar to Assumption 3 in [43], in which all the continuous signals $\alpha_i, i = 2, \ldots, n$ require some prior condition. Note that in this paper, we only need to know α_2. In this sense, we relax Assumption 3 in [43]. Assumption 5 is reasonable since the derivative of $p(v(t))$ for a practical system is always bounded when the actual signal $v(t)$ is determined [39], [44].

Based on the characterization of unknown dead-zone output, (2) can be rewritten as follows:

$$x_1 = g^{-1}(y) = \frac{1}{m}y + \frac{2b}{\pi}\arctan(ky) \quad (7)$$

where k is a positive design parameter. Differentiating x_1 with respect to y yields

$$\frac{dx_1}{dy} = \frac{1}{m} + \frac{2b}{\pi}\frac{k}{1 + (ky)^2} \quad (8)$$

Thus, we have $0 < \frac{1}{m} < \frac{dx_1}{dy}$, and further obtain $\dot{y} = \frac{dy}{dx_1}\dot{x}_1 = m(t)\dot{x}_1$ by defining $m(t) = \frac{dy}{dx_1}$ with $0 < m(t) < m$.

Remark 2: The expression in (7) represents the certainty equivalence dead-zone inverse. If we increase the design parameter k, we can employ this smooth model to approximate the nonsmooth symmetric dead-zone nonlinearity in (2). By differentiation $\frac{dx_1}{dy}$, we obtain a relationship between $\frac{dy}{dt}$ and $\frac{dx_1}{dt}$ to be used in the DSC technique.

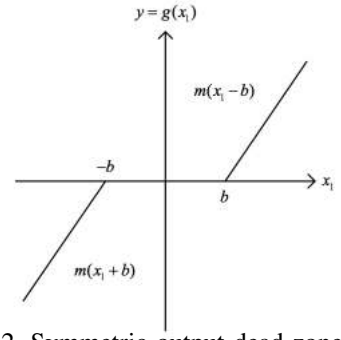

Figure 2. Symmetric output dead-zone model

A. Nussbaum Function Properties

In this paper, Nussbaum functions are used to handle the singularity problem of discontinuity function.

A function $N(\zeta)$ is defined as a Nussbaum-type function if it carries the following properties:

$$\lim_{s\to+\infty}\sup\frac{1}{s}\int_0^s N(\zeta)d\zeta = +\infty \quad (9)$$

$$\lim_{s\to-\infty}\inf\frac{1}{s}\int_0^s N(\zeta)d\zeta = -\infty \quad (10)$$

Commonly used Nussbaum functions are $\zeta^2\cos(\zeta)$ and $e^{\zeta^2}\cos(\frac{\pi}{2}\zeta)$, which are known as the even Nussbaum functions. As in [30], we use $N(\zeta)=e^{\zeta^2}\cos(\frac{\pi}{2}\zeta)$ in this paper to deal with unknown dead-zone output.

The following two lemmas associated with Nussbaum functions are needed in the stable controller design procedure.

Lemma 1 [30]: Let $V(\cdot)$ and $\zeta(\cdot)$ be smooth functions defined on $[0,t_f)$ with $V(t)\geq 0$, for all $t\in[0,t_f)$ and $N(\cdot)$ be an even smooth Nussbaum-type function. If the following inequality holds:

$$V(t)\leq c_0+e^{-c_1t}\int_0^t g(x(\tau))N(\zeta)\dot{\zeta}e^{c_1\tau}d\tau + e^{-c_1t}\int_0^t \dot{\zeta}e^{c_1\tau}d\tau, t\in[0,t_f) \quad (11)$$

where c_0 represents some suitable constant, c_1 is a positive constant, and $g(x(\tau))$ is a time-varying parameter which takes values in the unknown closed intervals $I:=[l^{-1},l^{+1}]$, with $0\notin I$, then $V(t),\zeta(t)$ and $\int_0^t g(x(\tau))N(\zeta)\dot{\zeta}d\tau$ must be bounded on $[0,t_f)$.

Lemma 2 (Young's inequality): The following inequality holds for any vectors $x,y\in R^n$

$$x^Ty\leq\frac{\varepsilon^p\parallel x\parallel^p}{p}+\frac{\parallel y\parallel^q}{q\varepsilon^q}$$

where $\varepsilon>0, p>1, q>1$ and $(p-1)(q-1)=1$.

B. Nonlinear Function Approximation

The capability of learning and continuous function approximation has made neural networks most useful in modeling highly uncertain and complex systems. In this paper, we employ RBFNNs to approximate any unknown smooth function $\varphi(Z)$ from R^q to R over a compact set Ω_Z as follows:

$$\varphi(Z)=W^{*\mathrm{T}}S(Z)+\delta(Z), Z\in\Omega_Z\in R^q$$

where W^* is an unknown ideal constant weight vector defined as $W^*:\arg\min_{\hat{W}\in R^l}\sup_{Z\in\Omega_Z}[\parallel\varphi(Z)-\hat{W}^TS(Z)\parallel]$ with $\hat{W}$ being the estimation of the optimal weight vector. Note that the actual value of the ideal constant weight vector W^* is not necessary, it is only required for the purposes of analysis of closed-loop stability and boundedness. $\delta(Z)$ is the optimal approximation error. $S(Z)=[s_1(Z),\ldots,s_l(Z)]^{\mathrm{T}}\in R^l$ is the basis function vector with $l>1$ being the neural network nodes

$$s_i(Z)=e^{-(Z-v_i)^T(Z-v_i)/k^2} \quad (12)$$

where $v_i=[\mu_{i1},\ldots,\mu_{iq_i}]^{\mathrm{T}}\in R^{q_i}$ is the center of the receptive field, and $k>0$ is the width of the Gaussian function. Define $s:=\frac{1}{2}\min_{i\neq j}\parallel v_i-v_j\parallel$, then the following inequality holds:

$$\parallel S(Z)\parallel\leq\sum_{j=0}^{\infty}3q(j+2)^{q-1}e^{\frac{-2s^2j^2}{k^2}} \quad (13)$$

In this paper, we use n RBFNNs to approximate n unknown smooth functions $H_i(Z_i)$

$$H_i(Z_i)=W_i^*\xi_i(Z_i)+\delta_i(Z_i), Z_i\in\Omega_{Z_i}\in R^{q_i} \quad (14)$$

where $Z_1=[x_1,s_1,\hat{\lambda},\dot{y}_d]^{\mathrm{T}}$, $Z_i=[\bar{x}_i,s_i,\dot{z}_i,\hat{\lambda}]^{\mathrm{T}}$. The modified basis function vector is $\xi_i(Z_i)=[\xi_{i,1}(Z_i),\ldots,\xi_{i,li}(Z_i)]^{\mathrm{T}}\in R^{li}$, $\xi_{ij}(Z_i)=\exp\left[-\frac{(Z_i-v_{ij})^{\mathrm{T}}(Z_i-v_{ij})}{k_{ij}^2}\right]$, $j=1,\ldots,l_i$, $i=1,\ldots,n$, and $v_{ij}=[v_{ij1},\ldots,vijq_{ij}]^{\mathrm{T}}$.

Remark 3: While RBFNN-based approximator is used here, it can be replaced by other unknown continuous function approximators such as fuzzy logic systems, wavelet neural networks, and multi-layer neural networks.

III. Main Results

In this section, we present an adaptive neural output-constrained tracking control scheme for system (1) using the barrier Lyapunov function (BLF) method and dynamic surface control technique. The design procedure contains n steps. Construct the BLF V_1 and the quadratic function V_i in advance as

$$V_1=\frac{1}{2}\log\frac{k_{b1}^2}{k_{b1}^2-s_1^2} \quad (15)$$

$$V_i=\frac{1}{2}s_i^2 \quad (16)$$

and the feasible adaptive neural tracking controllers are constructed as

$$\alpha_2=N(\zeta)(k_1s_1+\frac{k_{b1}^2-s_1^2}{2b_1^2}s_1\hat{\lambda}\xi_1^{\mathrm{T}}(Z_1)\xi_1(Z_1)) \quad (17)$$

$$\alpha_{i+1}=-k_is_i-\frac{1}{2b_i^2}s_i\hat{\lambda}\xi_i^{\mathrm{T}}(Z_i)\xi_i(Z_i) \quad (18)$$

$$\dot{\hat{\lambda}}=\sum_{i=1}^{n}\frac{1}{2b_i^2}s_i^2\hat{\lambda}\xi_i^{\mathrm{T}}(Z_i)\xi_i(Z_i)-\gamma\sigma\hat{\lambda} \quad (19)$$

where $i=2,\ldots,n-1$, and $k_1>\frac{1}{2}$, $b_1,b_i,k_i,\gamma,\sigma$ are the positive parameters given by the designer. The auxiliary Nussbaum parameter ζ is updated through solving the following differential equation: $\dot{\zeta}=\frac{k_1s_1^2}{k_{b1}^2-s_1^2}+\frac{1}{2b_1^2}s_1^2\hat{\lambda}\xi_1^{\mathrm{T}}(Z_1)\xi_1(Z_1)$, and the variable $\hat{\lambda}$ is the adaptive parameter which is specified as the estimate of the unknown constant λ as follows

$$\lambda=\max\{\|W_i^*\|^2,i=1,\ldots,n\}$$

Lemma 3: For the state vector $x=[x_1,\ldots,x_n]^T\in R^n$, the following holds:

$$\|x\|\leq\sum_{l=1}^{n}\rho_l\,|s_l|+\varphi(\bar{y}_n)+P^* \quad (20)$$

with $\rho_l=k_l+1+\frac{1}{2b_l^2}\hat{\lambda}$, for $l=2,\ldots,n-1$, $\rho_n=1$, and $P^*=\frac{1}{m}d^*+b$.

Proof: From (7), we have $|x_1|=|\frac{1}{m}y+\frac{2b}{\pi}\arctan(ky)|\leq\frac{1}{m}|y|+b$. Furthermore, by integrating (4)-(6) with Assumption

1, and using $\sum_{i=2}^{n}|y_i| \le \varphi(\bar{y}_n)$ with $\varphi(\bar{y}_n)$ being a nonnegative continuous function, we obtain the following result

$$\begin{aligned}\|x\| &\le \sum_{i=1}^{n}|x_i| = |x_1| + \sum_{i=2}^{n}|x_i| \\ &\le \frac{1}{m}|s_1 + y_d| + b + \sum_{i=2}^{n}|s_i + y_i + \alpha_i| \\ &\le \frac{1}{m}|s_1| + \frac{1}{m}d^* + b + \sum_{i=2}^{n}|s_i| + \varphi(\bar{y}_n) + \sum_{i=2}^{n}|\alpha_i| \end{aligned} \tag{21}$$

In view of Assumption 4 and (13), and considering the virtual control in (17), (18), the term $\sum_{i=2}^{n}|\alpha_i|$ is transformed into the following inequality

$$\begin{aligned}\sum_{i=2}^{n}|\alpha_i| &\le |\alpha_2| + \sum_{i=3}^{n}|\alpha_i| \\ &\le \rho_1|s_1| + \sum_{i=3}^{n}(k_{i-1} + \frac{1}{2b_{i-1}^2}\hat{\lambda})|s_{i-1}| \end{aligned} \tag{22}$$

Substituting (22) into (21), we have

$$\|x\| \le \sum_{l=1}^{n}\rho_l|s_l| + \varphi(\bar{y}_n) + P^* \tag{23}$$

A. Adaptive Neural Dynamic Surface Controller Design

In this subsection, we propose a design procedure for system (1). In each step, we design a virtual control function α_i and the first-order filter by using an appropriate Lyapunov function V_i. In the last step, a control law v is designed. Finally, we show that the designed adaptive neural controller solve the problem of tracking control for system (1) without violating the output constraints. In the following, for clarity, we define the notation:

$$\bar{s}_i = [s_1, ..., s_i]^{\mathrm{T}},\ \bar{y}_j = [y_2, ..., y_j]^{\mathrm{T}} \tag{24}$$

where $i = 1, \ldots, n$, $j = 2, \ldots, n$.

Step 1: The derivative of s_1 along with the conclusion of output dead-zone, and the first subsystem of (1) is

$$\begin{aligned}\dot{s}_1 &= m(t)\dot{x}_1 - \dot{y}_d \\ &= m(t)x_2 + m(t)f_1(x) + m(t)d_1(x,t) - \dot{y}_d \end{aligned} \tag{25}$$

In order to obtain a new filter variable z_2, we pass the virtual control signal α_2 through a first-order filter with a small positive time constant τ_2

$$\tau_2\dot{z}_2 + z_2 = \alpha_2,\ z_2(0) = \alpha_2(0) \tag{26}$$

Differentiating V_1 with respect to time t, applying (25), (5), (6) and Assumption 2, we obtain

$$\begin{aligned}\dot{V}_1 = \frac{s_1\dot{s}_1}{k_{b1}^2 - s_1^2} &\le \frac{m(t)s_1(s_2 + y_2 + \alpha_2)}{k_{b1}^2 - s_1^2} \\ &+ \frac{m(t)s_1\phi_1(\|x\|)}{k_{b1}^2 - s_1^2} + \frac{m(t)d_1(x,t)s_1}{k_{b1}^2 - s_1^2} - \frac{s_1\dot{y}_d}{k_{b1}^2 - s_1^2} \end{aligned} \tag{27}$$

Furthermore, by using Young's inequality, we have

$$\frac{m(t)s_1s_2}{k_{b1}^2 - s_1^2} \le \frac{m^2s_1^2}{2(k_{b1}^2 - s_1^2)^2} + \frac{1}{2}s_2^2 \tag{28}$$

$$\frac{m(t)s_1y_2}{k_{b1}^2 - s_1^2} \le \frac{m^2s_1^2}{2(k_{b1}^2 - s_1^2)^2} + \frac{1}{2}y_2^2 \tag{29}$$

$$\frac{m(t)d_1(x,t)s_1}{k_{b1}^2 - s_1^2} \le \frac{m^2\chi_1^2(x_1)s_1^2}{4(k_{b1}^2 - s_1^2)^2} + p_1^{*2} \tag{30}$$

Next, consider the increasing property of $\phi_1(\cdot)$, for the term $m(t)s_1\phi_1(\|x\|)/(k_{b1}^2 - s_1^2)$, it follows from the variable separation technique that

$$\begin{aligned}&\frac{m(t)s_1\phi_1(\|x\|)}{k_{b1}^2 - s_1^2} \le \frac{m|s_1|\,\phi_1(\sum_{l=1}^{n}\rho_l|s_l| + \varphi(\bar{y}_n) + P^*)}{k_{b1}^2 - s_1^2} \\ &\le \sum_{l=1}^{n}\frac{|s_1|m}{k_{b1}^2 - s_1^2}\phi_1((n+2)|s_l|\rho_l) \\ &+ \frac{m|s_1|}{k_{b1}^2 - s_1^2}\phi_1((n+2)\varphi(\bar{y}_n)) + \frac{m|s_1|}{k_{b1}^2 - s_1^2}\phi_1((n+2)P^*) \\ &\le \sum_{l=1}^{n}s_l^2\bar{\phi}_1^2 + \frac{m^2}{2a_1^2(k_{b1}^2 - s_1^2)^2}s_1^2\phi_1^2((n+2)\varphi(\bar{y}_n)) \\ &+ \frac{m^2s_1^2}{4(k_{b1}^2 - s_1^2)^2} + \frac{m^2}{2a_1^2(k_{b1}^2 - s_1^2)^2}s_1^2\phi_1^2((n+2)P^*) + a_1^2 \end{aligned} \tag{31}$$

where $\bar{\phi}_1^2 = (n+2)^2\rho_l^2q_1^2((n+2)|s_l|\rho_l)$ with $q_1(\cdot)$ being a smooth function. Taking the virtual control (17) and (28)-(31) into account, (27) can be rewritten as

$$\begin{aligned}\dot{V}_1 \le &-k_1\frac{s_1^2}{k_{b1}^2 - s_1^2} + \frac{1}{2}s_2^2 + \frac{1}{2}y_2^2 + (m(t)N(\zeta) + 1)\dot{\zeta} \\ &+ \frac{5m^2s_1^2}{4(k_{b1}^2 - s_1^2)^2} + \frac{m^2s_1^2}{2a_1^2(k_{b1}^2 - s_1^2)^2}\phi_1^2((n+2)\varphi(\bar{y}_n)) \\ &+ \frac{m^2s_1^2}{2a_1^2(k_{b1}^2 - s_1^2)^2}\phi_1^2((n+2)P^*) - \frac{1}{2b_1^2}s_1^2\hat{\lambda}\xi^{\mathrm{T}}(Z_1)\zeta(Z_1) \\ &+ \frac{m^2\chi_1^2(x_1)s_1^2}{4(k_{b1}^2 - s_1^2)^2} - \frac{s_1\dot{y}_d}{k_{b1}^2 - s_1^2} + \sum_{l=1}^{n}s_l^2\bar{\phi}_1^2 + a_1^2 + p_1^{*2} \end{aligned} \tag{32}$$

Remark 4: It follows from (25) that the main design difficulties lie in two facts: the unknown dead-zone time-varying coefficient $m(t)$ and the unknown subsystem function term $f_1(x)$ including whole state variables. Both cannot appear in the controller or be directly approximated by RBFNNs. We solve these design difficulties as follows. Equations (28)-(32) effectively tackle the issue of $m(t)$ by using Young's inequality and Nussbaum-type functions. Equations (21)-(23) deduce the relationship between $\|x\|$ and $|s_l|, l = 1, \ldots, n$, which can be used to decompose $f_1(x)$ into a series of continuous functions by employing the variable separation technique with the Young's inequality in (31). The uncertain term $\sum_{l=1}^{n}s_l^2\bar{\phi}_1^2$ in (32) contains not only the current variable s_1, but also all the subsequent variables $s_2, \ldots, s_n$. This uncertain term will be completely approximated by the use of RBFNNs in the sequel.

Step i: $(2 \le i \le n-1)$ Considering the ith equation of system (1) and noting (5), we obtain

$$\dot{s}_i = x_{i+1} + f_i(x) + d_i(x,t) - \dot{z}_i \tag{33}$$

Let α_{i+1} pass through the ith low pass first-order filter with small time constants $\tau_{i+1} > 0$. Then, the ith filtered virtual control signal z_{i+1} is obtained, namely,

$$\tau_{i+1}\dot{z}_{i+1} + z_{i+1} = \alpha_{i+1}, z_{i+1}(0) = \alpha_{i+1}(0) \tag{34}$$

We consider the Lyapunov candidate function $V_i = \frac{1}{2}s_i^2$. Proceeding similarly to take the derivative of V_i, and substitute (33), (5), (6) into $\dot{V}_i$, we obtain

$$\begin{aligned}\dot{V}_i = \quad & \dot{s}_i s_i \le s_i(s_{i+1} + y_{i+1} + \alpha_{i+1} \\ & + f_i(x) + d_i(x,t) - \dot{z}_i) \end{aligned} \tag{35}$$

Based on Assumption 2, we obtain $s_i f_i(x) \le |s_i|\phi_i(\|x\|)$. By invoking Lemma 2 and using (20), we have

$$\begin{aligned} & |s_i|\,\phi_i(\|x\|) \le |s_i|\,\phi_i(\sum_{l=1}^{n}\rho_l\,|s_l| + \varphi(\bar{y}_n) + P^*) \\ & \le \sum_{l=1}^{n}|s_i|\phi_i((n+2)\,|s_l|\,\rho_l) + |s_i|\,\phi_i((n+2)\varphi(\bar{y}_n)) \\ & + |s_i|\,\phi_i((n+2)P^*) \\ & \le \sum_{l=1}^{n} s_l^2\bar{\phi}_i^2 + \frac{s_i^2}{4} + \frac{1}{2a_i^2}s_i^2\phi_i^2((n+2)\varphi(\bar{y}_n)) \\ & + \frac{1}{2a_i^2}s_i^2\phi_i^2((n+2)P^*) + a_i^2 \end{aligned} \tag{36}$$

where $\bar{\phi}_i^2 = (n+2)^2\rho_l^2 q_i^2((n+2)\,|s_l|\,\rho_l)$ with $q_i(\cdot)$ being a smooth function. We consider (18), (36) and use Young's inequalities. Then, (35) can be written as follows

$$\begin{aligned} \dot{V}_i \le & -k_i s_i^2 + \frac{1}{2}s_{i+1}^2 + \frac{1}{2}y_{i+1}^2 - \frac{1}{2b_i^2}s_i^2\hat{\lambda}\xi_i^{\mathrm{T}}(Z_i)\zeta(Z_i) \\ & + \frac{5}{4}s_i^2 + \frac{1}{2a_i^2}s_i^2\phi_i^2((n+2)\varphi(\bar{y}_n)) + \frac{1}{4}\chi_i^2(\bar{x}_i)s_i^2 + p_i^{*2} \\ & + \frac{1}{2a_i^2}s_i^2\phi_i^2((n+2)P^*) - s_i\dot{z}_i + \sum_{l=1}^{n}s_l^2\bar{\phi}_i^2 + a_i^2 \end{aligned} \tag{37}$$

Step n**:** The time derivative of (5) $(k = n)$ along nth subsystem can be represented by $\dot{s}_n = u(v(t)) + f_n(x) + d_n(x,t) - \dot{z}_n$. We consider the Lyapunov candidate function $V_n = \frac{1}{2}s_n^2$ and by the redefined saturation nonlinearity in (3), we obtain

$$\dot{V}_n = s_n(p_{v^\mu}v(t) + \Delta v(t) + f_n(x) + d_n(x,t) - \dot{z}_n)$$

The actual control law is proposed as follows:

$$v(t) = -\frac{1}{g_m}(k_n s_n + \frac{1}{2b_n}s_n\hat{\lambda}\xi_n^{\mathrm{T}}(Z_n)\xi_n(Z_n)) \tag{38}$$

Using Young's inequality and Assumption 5, we have

$$p_{v^\mu}v(t)s_n \le -k_n s_n^2 - \frac{1}{2b_n^2}s_n^2\hat{\lambda}\xi_n^{\mathrm{T}}(Z_n)\xi_n(Z_n)$$

$$\Delta(v(t))s_n \le \frac{1}{2}s_n^2 + \frac{1}{2}\bar{d}^2$$

Proceeding similarly, we obtain

$$\begin{aligned} \dot{V}_n \le & -k_n s_n^2 - \frac{1}{2b_n^2}s_n^2\hat{\lambda}\xi_n^{\mathrm{T}}(Z_n)\zeta(Z_n) + \frac{3}{4}s_n^2 \\ & + \frac{1}{2a_n^2}s_n^2\phi_n^2((n+2)\varphi(\bar{y}_n)) + \frac{1}{2a_n^2}s_n^2\phi_n^2((n+2)P^*) \\ & + \frac{1}{4}s_n^2\chi_n^2(x) - s_n\dot{z}_n + \sum_{l=1}^{n}s_l^2\bar{\phi}_n^2 + a_n^2 + p_n^{*2} \end{aligned} \tag{39}$$

Based on the above discussions, a flow diagram capturing the procedure for the controller design is given in Fig. 3.

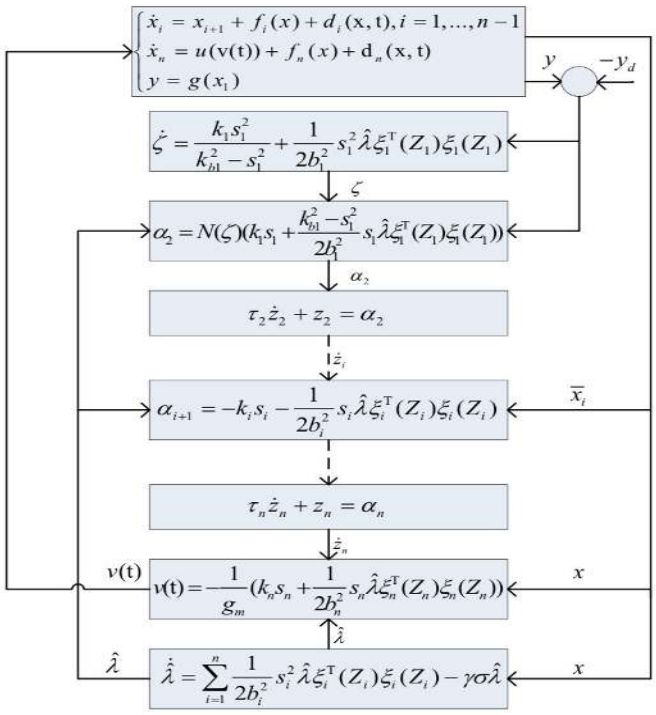

Figure 3. Flow diagram of the adaptive neural control scheme

B. Stability Analysis

The purpose of this subsection is to validate that the proposed adaptive neural controllers of system (1) can achieve semi-global uniformly ultimately boundedness and prescribed error bound. To this end, we first define some compact sets as follows:

$$\begin{aligned} \Omega_i &= \{[\bar{s}_i, \bar{y}_{i+1}, \hat{\lambda}]^{\mathrm{T}} : V_i \le p\} \subset \mathbf{R}^{p_i}, i = 1,...,n \\ \Omega_d &= \{[y_d, \dot{y}_d, \ddot{y}_d]^{\mathrm{T}} : y_d^2 + \dot{y}_d^2 + \ddot{y}_d^2 \le \varsigma\} \subset R^3 \end{aligned}$$

where ς is a positive constants, $p > 0$ is a design constant, $p_i = 2i+1$, $i = 1,\ldots,n$, and

$$V_1 = \frac{1}{2}\log\frac{k_{b1}^2}{k_{b1}^2 - s_1^2} + \frac{\tilde{\lambda}^2}{2\gamma} \tag{40}$$

$$\begin{aligned} V_i = & \frac{1}{2}\log\frac{k_{b1}^2}{k_{b1}^2 - s_1^2} + \sum_{j=2}^{i}\frac{s_j^2}{2} \\ & + \sum_{j=2}^{i}\frac{y_j^2}{2} + \frac{\tilde{\lambda}^2}{2\gamma}, i = 2,\cdots,n \end{aligned} \tag{41}$$

For the analysis of stability, choose the total Lyapunov candidate function V as

$$V = V_n = \frac{1}{2}\log\frac{k_{b1}^2}{k_{b1}^2 - s_1^2} + \sum_{j=2}^{i}\frac{s_j^2}{2} + \sum_{j=2}^{i}\frac{y_j^2}{2} + \frac{\tilde{\lambda}^2}{2\gamma} \tag{42}$$

It is easy to see that $\Omega_n \times \Omega_d$ is also a compact in R^{p_n+3}. Furthermore, $\|\eta_j\|$ has a maximum m_j and on $\Omega_n \times \Omega_d$, and $\|\psi_i\|$ has a maximum h_i and on $\Omega_n \times \Omega_d$, $j = 2,\ldots,n$, $i = 1,\ldots,n$. There exists a positive constant Y^* such that $\|\varphi(\bar{y}_n)\| \le Y^*$ on Ω_n.

Based on above, we are ready to present our main result.

Theorem 1: Consider the closed-loop output-constrained nonstrict-feedback system consisting of system (1) under Assumptions 1-5. Define a compact set as $\Omega_{k_{b1}} := \{s_1(t) \in R||s_1| < k_{b1}\}$. If the initial condition satisfies $s_1(0) \in \Omega_{k_{b1}}$, and the virtual control laws are employed in (17) and (18), the actual control law and adaptation law are designed in (38) and (19), then, there exist positive constants $k_i, \tau_i, \gamma, \sigma$ such that the output constraint $s_1(t) \in \Omega_{k_{b1}}$ never be violated, all the other signals are semi-global uniformly ultimately bounded, and k_i and τ_i satisfy

$$\begin{cases} k_1 \geq \frac{1}{2} + \alpha_0 \\ k_i \geq 1 + \frac{1}{2}\alpha_0 \\ \frac{1}{\tau_{i+1}} \geq \frac{3}{2} + \frac{1}{2}\alpha_0 \\ \alpha_0 \leq \gamma\sigma \end{cases} \tag{43}$$

Proof: From (6) along (26) and (34), we obtain the derivative of boundary layer errors as:

$$\dot{y}_{i+1} = -\frac{y_{i+1}}{\tau_{i+1}} - \dot{\alpha}_{i+1}$$

where $i = 1, \ldots, n-1$, by using (17) and (18), we have

$$\begin{aligned} y_{i+1}\dot{y}_{i+1} &\leq -\frac{y_{i+1}^2}{\tau_{i+1}} + |y_{i+1}|\,\eta_{i+1} \\ &\leq -\frac{y_{i+1}^2}{\tau_{i+1}} + y_{i+1}^2 + \frac{\eta_{i+1}^2}{4} \end{aligned} \tag{44}$$

with

$$\begin{aligned} |\dot{\alpha}_2| = |&-\frac{dN(\zeta)}{d\zeta}[\dot{\zeta}k_1 s_1 + \frac{k_{b1}^2 - s_1^2}{2b_1^2}s_1\hat{\lambda}\xi_1^{\mathrm{T}}(Z_1)\xi_1(Z_1)] \\ &+N(\zeta)\frac{k_{b1}^2 s_1 - s_1^2\dot{s}_1}{2b_1^2}\hat{\lambda}\|\xi_1(Z_1)\|^2 \\ &-\frac{N(\zeta)(k_{b1}^2 - s_1^2)\|\xi_1(Z_1)\|^2\dot{s}_1\hat{\lambda}}{2b_1^2} \\ &-N(\zeta)[\frac{k_{b1}^2 - s_1^2}{2b_1^2}\|\xi_1(Z_1)\|^2 s_1\dot{\hat{\lambda}}] \\ &-N(\zeta)[\frac{k_{b1}^2 - s_1^2}{2b_1^2}s_1\hat{\lambda}\frac{d\|\xi_1(Z_1)\|^2}{dt}] \\ &-N(\zeta)k_1\dot{s}_1| \leq \eta_2(\bar{s}_n, \bar{y}_n, \hat{\lambda}, \zeta, y_d, \dot{y}_d, \ddot{y}_d) \\ |\alpha_{i+1}| = |&k_i\dot{s}_i + \frac{1}{2b_i^2}\dot{s}_i\hat{\lambda}\xi_i^{\mathrm{T}}(Z_i)\xi_i(Z_i) \\ &+\frac{1}{2b_i^2}s_i\dot{\hat{\lambda}}\|\xi_i(Z_i)\|^2 + \frac{1}{2b_i^2}s_i\hat{\lambda}\frac{d\|\xi_i(Z_i)\|^2}{dt}| \\ &\leq \eta_{i+1}(\bar{s}_n, \bar{y}_n, \hat{\lambda}, y_d, \dot{y}_d, \ddot{y}_d) \end{aligned}$$

where $\eta_{i+1}, i = 1, \ldots, n-1$ are nonnegative continuous functions.

Differentiating (42) and substituting (32), (37), (39) and (44) into $\dot{V}$, we have

$$\begin{aligned} \dot{V} = \sum_{i=1}^{n}\dot{V}_i \leq &-k_1\frac{s_1^2}{k_{b1}^2 - s_1^2} + \sum_{i=2}^{n}(\frac{1}{2} - k_i)s_i^2 \\ &+\sum_{i=1}^{n-1}(-\frac{1}{\tau_{i+1}} + \frac{3}{2})y_{i+1}^2 - \sum_{i=1}^{n}\frac{1}{2b_i^2}s_i^2\hat{\lambda}\xi_i^{\mathrm{T}}(Z_i)\zeta(Z_i) \\ &+(m(t)N(\zeta)+1)\dot{\zeta} + \frac{5m^2 s_1^2}{4(k_{b1}^2 - s_1^2)^2} + \frac{m^2\chi_1^2(x_1)s_1^2}{4(k_{b1}^2 - s_1^2)^2} \\ &+\sum_{i=2}^{n-1}\frac{5}{4}s_i^2 + \frac{3}{4}s_n^2 + \sum_{i=1}^{n}\frac{1}{2a_i^2}s_i^2\phi_i^2((n+2)Y^*) \\ &+\frac{m^2 s_1^2}{2a_1^2(k_{b1}^2 - s_1^2)^2}\phi_1^2((n+2)P^*) + \sum_{i=2}^{n}\frac{1}{4}\chi_i^2(\bar{x}_i)s_i^2 \\ &+\sum_{i=2}^{n}\frac{1}{2a_i^2}s_i^2\phi_i^2((n+2)P^*) \\ &+\sum_{i=1}^{n}\sum_{l=1}^{n}s_l^2\bar{\phi}_i^2 - \sum_{i=2}^{n}s_i\dot{z}_i - \frac{s_1\dot{y}_d}{k_{b1}^2 - s_1^2} \\ &+\sum_{i=1}^{n}a_i^2 + \sum_{i=1}^{n-1}\frac{1}{4}\eta_{i+1}^2 + \sum_{i=1}^{n}p_i^{*2} - \frac{\tilde{\lambda}\dot{\hat{\lambda}}}{\gamma} \end{aligned} \tag{45}$$

Then, we obtain the unknown black-box functions which will be approximated by RBFNNs later by rearranging the sequence as follows

$$\sum_{i=1}^{n}\sum_{l=1}^{n}s_l^2\bar{\phi}_i^2 = \sum_{i=1}^{n}s_i^2\sum_{j=1}^{n}\bar{\phi}_j^2 \tag{46}$$

where $\bar{\phi}_j^2 = (n+2)^2\rho_i^2 q_j^2((n+2)\,|s_i|\,\rho_i)$. Let

$$\begin{aligned} H_1(Z_1) = &\frac{5m^2 s_1}{4(k_{b1}^2 - s_1^2)^2} + \frac{m^2 s_1}{2a_1^2(k_{b1}^2 - s_1^2)^2}\phi_1^2((n+2)P^*) \\ &+\frac{1}{2a_1^2}s_1\phi_1^2((n+2)Y^*) - \frac{\dot{y}_d}{k_{b1}^2 - s_1^2} + \frac{m^2\chi_1^2(x_1)s_1}{4(k_{b1}^2 - s_1^2)^2} \\ &+s_1\sum_{j=1}^{n}(n+2)^2\rho_1^2 q_j^2((n+2)\,|s_1|\,\rho_1) \end{aligned} \tag{47}$$

$$\begin{aligned} H_i(Z_i) = &\frac{5}{4}s_i + \frac{1}{2a_i^2}s_i\phi_i^2((n+2)P^*) + \frac{1}{2a_i^2}s_i\phi_i^2((n+2)Y^*) \\ &-\dot{z}_i + s_i\sum_{j=1}^{n}(n+2)^2\rho_i^2 q_j^2((n+2)\,|s_i|\,\rho_i) \\ &+\frac{1}{4}\chi_i^2(\bar{x}_i)s_i, i = 2, ..., n-1 \end{aligned} \tag{48}$$

$$\begin{aligned} H_n(Z_n) = &\frac{3}{4}s_n + \frac{1}{2a_n^2}s_n\phi_n^2((n+2)P^*) \\ &+\frac{1}{2a_n^2}s_n\phi_n^2((n+2)Y^*) - \dot{z}_n + \frac{1}{4}\chi_n^2(x)s_n \\ &+s_n\sum_{j=1}^{n}(n+2)^2\rho_n^2 q_j^2((n+2)\,|s_n|\,\rho_n) \end{aligned} \tag{49}$$

It follows from taking (45), together with (46)-(49), into account that

$$\begin{aligned} \dot{V} \leq &-k_1\frac{s_1^2}{k_{b1}^2 - s_1^2} + \sum_{i=2}^{n}(\frac{1}{2} - k_i)s_i^2 \\ &+\sum_{i=1}^{n-1}(-\frac{1}{\tau_{i+1}} + \frac{3}{2})y_{i+1}^2 - \sum_{i=1}^{n}\frac{1}{2b_i^2}s_i^2\hat{\lambda}\xi_i^{\mathrm{T}}(Z_i)\zeta(Z_i) \\ &+(m(t)N(\zeta)+1)\dot{\zeta} + \sum_{i=1}^{n}s_i H_i(Z_i) \\ &+\sum_{i=1}^{n}a_i^2 + \sum_{i=1}^{n-1}\frac{1}{4}\eta_{i+1}^2 + \sum_{i=1}^{n}p_i^{*2} - \frac{\tilde{\lambda}\dot{\hat{\lambda}}}{\gamma} \end{aligned} \tag{50}$$

Next, we observe that it is feasible to use RBFNNs to approximate the unknown nonlinear functions $H_i(Z_i), i = 1,\ldots,n$ on the compact set Ω_{Z_i}. Then, the above inequality (50) becomes

$$\begin{aligned}\dot{V} \le & \sum_{i=1}^{n} s_i(W_i^*\xi_i(Z_i)+\delta_i(Z_i)) - k_1\frac{s_1^2}{k_{b1}^2-s_1^2} \\ & + \sum_{i=2}^{n}(\frac{1}{2}-k_i)s_i^2 + (m(t)N(\zeta)+1)\dot{\zeta} \\ & + \sum_{i=1}^{n-1}(-\frac{1}{\tau_{i+1}}+\frac{3}{2})y_{i+1}^2 - \sum_{i=1}^{n}\frac{1}{2b_i^2}s_i^2\hat{\lambda}\xi_i^{\mathrm{T}}(Z_i)\zeta(Z_i) \\ & + \sum_{i=1}^{n}a_i^2 + \sum_{i=1}^{n-1}\frac{1}{4}\eta_{i+1}^2 + \sum_{i=1}^{n}p_i^{*2} - \frac{\tilde{\lambda}\dot{\hat{\lambda}}}{\gamma} \end{aligned} \tag{51}$$

with

$$\begin{aligned} s_iW_i^*\xi_i(Z_i) &\le \frac{1}{2b_i^2}s_i^2\lambda\xi_i^{\mathrm{T}}(Z_i)\xi_i(Z_i)+\frac{1}{2}b_i^2 \\ s_i\delta_i(Z_i) &\le |s_i|\,|\delta_i(Z_i)| \\ &\le \frac{1}{2}s_i^2+\frac{1}{2}\psi_i^2(\bar{s}_n,\bar{y}_n,\hat{\lambda},y_d,\dot{y}_d) \end{aligned} \tag{52}$$

where continuous functions $\psi_i(\bar{s}_n,\bar{y}_n,\hat{\lambda},y_d,\dot{y}_d)$ satisfy

$$|\delta_i(Z_i)| \le \psi_i(\bar{s}_n,\bar{y}_n,\hat{\lambda},y_d,\dot{y}_d) \tag{53}$$

Denote $\tilde{\lambda} = \lambda - \hat{\lambda}$. Substituting (52) and (19) into (51) yields

$$\begin{aligned}\dot{V} \le & -(k_1-\frac{1}{2})\frac{s_1^2}{k_{b1}^2-s_1^2} + \sum_{i=2}^{n}(1-k_i)s_i^2 \\ & + \sum_{i=1}^{n-1}(-\frac{1}{\tau_{i+1}}+\frac{3}{2})y_{i+1}^2 + (m(t)N(\zeta)+1)\dot{\zeta} \\ & + \sum_{i=1}^{n-1}\frac{1}{4}\eta_{i+1}^2 + \sum_{i=1}^{n}\frac{1}{2}\psi_i^2 + \sum_{i=1}^{n}\frac{1}{2}b_i^2 \\ & + \sum_{i=1}^{n}p_i^{*2} + \sum_{i=1}^{n}a_i^2 - \sigma\tilde{\lambda}\hat{\lambda} \end{aligned} \tag{54}$$

Since $-\sigma\tilde{\lambda}\hat{\lambda} = -\sigma\tilde{\lambda}(\tilde{\lambda}+\lambda) \le \sigma(\frac{1}{2}\lambda^2 - \frac{1}{2}\tilde{\lambda}^2)$ and $-s_1^2/k_{b1}^2 - s_1^2 \le -\log(k_{b1}^2/k_{b1}^2-s_1^2)$ in the set $|s_1| < k_{b1}$, subsequently

$$\dot{V} \le -\alpha_0 V + \mu + (m(t)N(\zeta)+1)\dot{\zeta} \tag{55}$$

where $\mu = 1/4\sum_{i=2}^{n}m_i^2 + 1/2\sum_{i=1}^{n}h_i^2 + 1/2\sum_{i=1}^{n}b_i^2 + \sum_{i=1}^{n}a_i^2 + \sigma\lambda^2/2 + \sum_{i=1}^{n}p_i^{*2}$. Multiplying (55) by $e^{\alpha_0 t}$ and integrating it over $[0,t]$ yields

$$V \le c + e^{-\alpha_0 t}\int_0^t (m(t)N(\zeta)+1)\dot{\zeta}e^{\alpha_0\tau}d\tau \tag{56}$$

where $c = V(0) + \mu/\alpha_0$. From Lemma 1, it follows that $V, \int_0^t (m(t)N(\zeta)+1)\dot{\zeta}e^{\alpha_0\tau}d\tau$ and ζ remain bounded on $[0,t)$. Furthermore, the result can be extended to $t \to \infty$. Therefore, all signals in the closed-loop are SGUUB.

Let $e^{-\alpha_0 t}\int_0^t (m(t)N(\zeta)+1)\dot{\zeta}e^{\alpha_0\tau}d\tau \le c_0$. Then, we have

$$\frac{1}{2}\log\frac{k_{b1}^2}{k_{b1}^2-s_1^2} \le V \le d \tag{57}$$

where $d = c + c_0$. Multiplying (57) by $(k_{b1}^2 - s_1^2)$ further yields

$$|s_1| \le k_{b1}\sqrt{1-e^{-2d}} \tag{58}$$

As a consequence, the tracking error $s_1(t)$ never exceeds the output constraint k_{b1}, and achieves arbitrarily small value by adjusting the design parameters. The proof of Theorem 1 is thus completed.

Remark 5: From (46), we observe that the term $\sum_{i=1}^{n}\sum_{l=1}^{n}s_l^2\bar{\phi}_i^2$ derived from uncertain system dynamics $f_i(x), i = 1,\ldots,n$ has been divided into n unknown continuous functions $s_i^2\sum_{j=1}^{n}\bar{\phi}_j^2, i = 1,\ldots,n$, which only contain current error surface of each subsystem. Thus, from (47)-(49), it becomes feasible to use RBFNNs to approximate these unknown continuous functions in each step.

Remark 6: We note that the methods in [3], [19]−[22] require repeated differentiation of virtual controllers, leading to an ever-increasing dimension of input vector of NNs/FLS with the growth of system order. From our derived algorithm, the filtered virtual controller $\dot{z}_i, i = 2,\ldots,n$ has been introduced into the input vector $Z_i, i = 2,\ldots,n$ of each RBFNN. Thus, the dimension of input vector greatly reduces. Consequently, the required learning time significantly decreases.

Remark 7: In the developed adaptive DSC-based control scheme, we should lower the tracking error s_1 in (58) in order to obtain a good tracking performance, whose value depends on the initial conditions $s_1(0),\ldots,s_n(0)$, $\hat{\lambda}(0)$, λ as well as the design parameters $k_1,\ldots,k_n,\gamma,\sigma,b_1,\ldots,b_n,l_1,\ldots,l_n$. Since there is no analytical result in the literature to quantify the relationship of $l_1,\ldots,l_n$, λ, $\delta_1,\ldots,\delta_n$, an explicit computation expression of the stability condition is not available at present. Some suggestions are given to guide the choices of control parameters and initial conditions: (1) Decreasing σ helps to reduce μ, and will reduce the tracking error; (2) Decreasing initial values $s_1(0),\ldots,s_n(0)$ and increasing γ will help to reduce $V(0)$, subsequently result in the decrease of tracking error; and (3) Increasing the number of NN nodes l_i reduces δ_i in (14), and will improve both the performance and stability of the adaptive neural system. In addition, small δ_i reduces μ, subsequently the tracking error.

IV. Simulation Examples

We use a numerical example and two practical models to illustrate the feasibility and effectiveness of the proposed control method.

Example 1: Consider the following third-order nonlinear system with symmetric output dead-zone and input saturation

$$\begin{cases} \dot{x}_1 = x_2 + 2x_1\sin(x_1x_3) + x_1x_2 + 0.5x_1\sin(t) \\ \dot{x}_2 = x_3 + x_1^2 + x_1x_2 + x_2\cos(x_1) + 0.2\cos(0.5x_2) \\ \dot{x}_3 = u(v) + x_2x_3 + x_3\sin(x_1x_2) + 0.1\cos(x_2x_3) \\ y = g(x_1) \end{cases} \tag{59}$$

where $x = [x_1,x_2,x_3]^{\mathrm{T}} \in R^3$ is the state variables. $y = g(x_1)$ is the system output and input of an unknown symmetric output dead-zone defined in (2). The output dead-zone parameters are chosen as $b = 0.3$ and $m = 1$. The saturation nonlinearity is characterized by the parameter $u_s = 15$. As

a result, system (59) is in the nonstrict-feedback form. The desired trajectory is given as $y_d = 0.5\sin(t)$, and the error is limited in the set $|s(t)| \le k_{b1} = 0.5$. According to Theorem 1, the virtual control laws (17) and (18), the control law (38) and the adaptive law (19) are chosen, respectively. The first-order filters are designed as (34).

For the neural network design, the basis function vector $\xi_i(Z_i) = [\xi_{i1}(Z_i), \ldots, \xi_{ili}(Z_i)]^{\mathrm{T}} \in R^{li}$ is obtained by calculating Gaussian function $\xi_{ij}(Z_i) = \exp\left[-\frac{(Z_i - v_{ij})^{\mathrm{T}}(Z_i - v_{ij})}{k_{ij}^2}\right]$, where $j = 1, \ldots, l_i$, $i = 1, 2, 3$. $l_1 = l_2 = 9, l_3 = 25$. $v_{1j} = (j-5)[1,1,1,1]^{\mathrm{T}}, j = 1, \ldots, l_1$, $v_{2j} = 0.5(j-5)[1,1,1,1,1]^{\mathrm{T}}, j = 1, \ldots, l_2$, $v_{3j} = 0.5(j-13)[1,1,1,1,1,1]^{\mathrm{T}}$, $j = 1, \ldots, l_3$. $Z_1 = [x_1, s_1, \hat{\lambda}, \dot{y}_d]^{\mathrm{T}}$, $Z_2 = [\bar{x}_2, s_2, \dot{z}_2, \hat{\lambda}]^{\mathrm{T}}$, $Z_3 = [\bar{x}_3, s_3, \dot{z}_3, \hat{\lambda}]^{\mathrm{T}}$.

The initial conditions are taken as $[x_1(0), x_2(0), x_3(0)]^{\mathrm{T}} = [0.5, 0, 0]^{\mathrm{T}}$, $\hat{\lambda}(0) = 0.5$, $z_2(0) = z_3(0) = 0.5$ and $\zeta(0) = 0.5$. The design parameters: $k_1 = 2, k_2 = 2, k_3 = 5$, $\gamma = 100, \sigma = 0.05$, $b_1 = b_2 = b_3 = 10$. The time constants of first-order filters: $\tau_2 = \tau_3 = 0.001$.

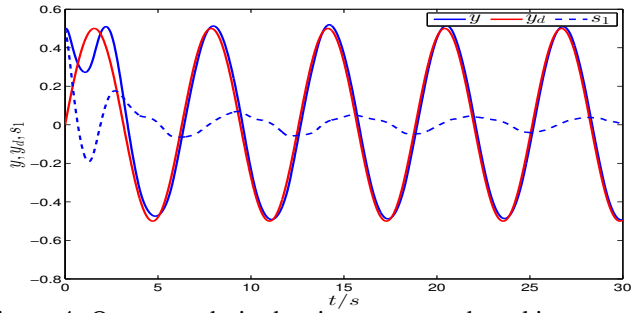

Figure 4. Output y, desired trajectory y_d and tracking error s_1 of Example 1

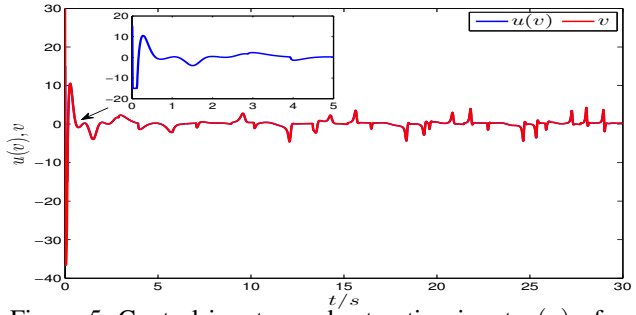

Figure 5. Control input v and saturation input $u(v)$ of Example 1

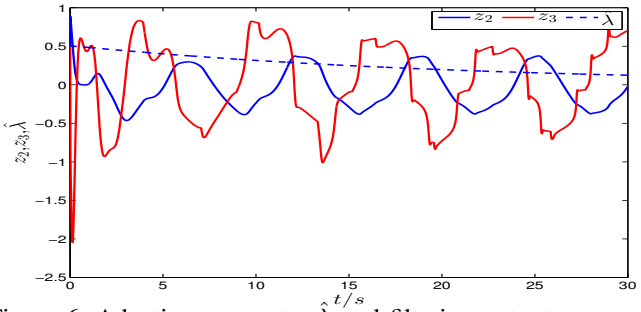

Figure 6. Adaptive parameter $\hat{\lambda}$ and filtering outputs z_2, z_3 of Example 1

The simulation results are shown in Figs. 4-7. From Fig. 4, we can see good tracking performance and the prescribed tracking error constraint $|s_1(t)| \le k_{b1}$ are achieved. The boundedness of control signal v, adaptive parameter $\hat{\lambda}$ and filtering virtual control z_2, z_3 are shown in Figs. 5 and 6.

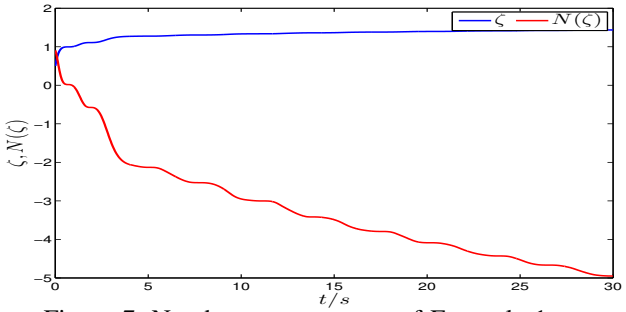

Figure 7. Nussbaum parameters of Example 1

Example 2: We consider a simplified Brusselator model describing a certain set of chemical reactions [45]

$$\begin{cases} \dot{x}_1 = a - (b+1)x_1 + x_1^2 x_2 \\ \dot{x}_2 = bx_1 - x_1^2 x_2 + (2 + \cos(x_1))u \\ y = x_1 \end{cases} \tag{60}$$

where x_1 and x_2 represent the concentrations of reaction intermediates. The constants $a, b > 0$ denote the supply of "reservoir" chemicals. According to [45], modeling error and other types of unknown nonlinearities exist in the practical chemical reactions. Therefore, the controlled Brusselator model with symmetric output dead-zone, input saturation and disturbance is assumed to be

$$\begin{cases} \dot{x}_1 = a - (b+1)x_1 + x_1^2 x_2 + d_1(x,t) \\ \dot{x}_2 = bx_1 - x_1^2 x_2 + (2 + \cos(x_1))u(v) + d_2(x,t) \\ y = g(x_1) \end{cases} \tag{61}$$

where $d_1(x,t) = 0.7x_1^2\cos(1.5t)$ and $d_2(x,t) = 0.5\sin(x_1 x_2)$ are disturbance terms. The unknown nonlinearities: $f_1(x) = a - (b+1)x_1 + (x_1^2 - 1)x_2$, $f_2(x) = bx_1 - x_1^2 x_2$. The deadzone parameters: $b = 0.8$, $m = 1$. The saturation parameter: $u_s = 10$. We can see that the Brusselator model (61) is in the form of (1) with dead-zone output (2) and saturation nonlinearity.

In the simulation, the input vector $Z_1 = [x_1, s_1, \hat{\lambda}, \dot{y}_d]^{\mathrm{T}}$ of the first neural networks contains 20 nodes (i.e. $l_1 = 1, \ldots, 20$), with centers v_{1j} evenly spaced in $[0.15, 3] \times [0.15, 3] \times [0.15, 3] \times [0.15, 3]$ and widths $k_{1j} = 1$, $j = 1, \ldots, l_1$. The input vector $Z_2 = [x_1, x_2, s_2, \hat{\lambda}, \dot{z}_2]^{\mathrm{T}}$ of the second neural networks contains 20 nodes (i.e., $l_2 = 1, \ldots, 20$), with centers v_{2j} evenly spaced in $[0.15, 3] \times [0.15, 3] \times [0.15, 3] \times [0.15, 3] \times [0.15, 3]$ and widths $k_{2j} = 1$, $j = 1, \ldots, l_2$. The aforementioned system parameters are given as $a = 1$, $b = 3$. We select the control parameters as $k_1 = 7$, $k_2 = 2$, $\gamma = 2$, $\sigma = 0.2$, $\tau_2 = 0.01$, $b_1 = b_2 = 10$. For the initial conditions, $[x_1(0), x_2(0)]^{\mathrm{T}} = [2.7, 1]^{\mathrm{T}}$, $\hat{\lambda}(0) = 0$, $z_2(0) = 4$, $\zeta(0) = 1$. Figs. 8-11 show the performance results of Example 2.

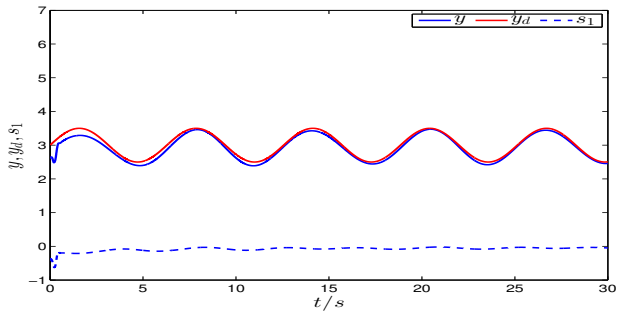

Figure 8. Output y, desired trajectory y_d and tracking error s_1 of Example 1

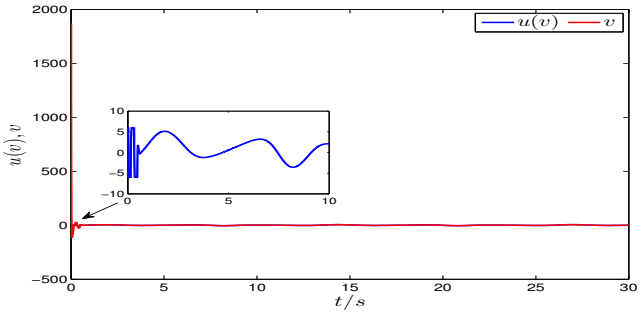

Figure 9. Control input v and saturation input $u(v)$ of Example 2

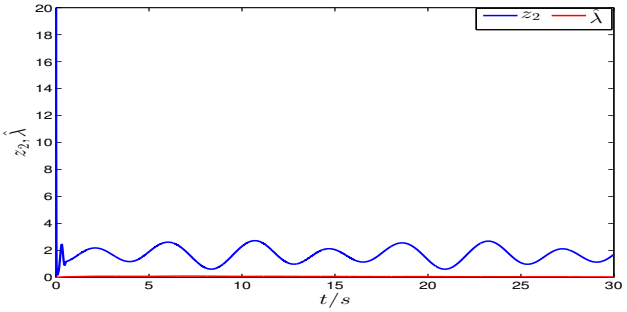

Figure 10. Adaptive parameter $\hat{\lambda}$ and filtering output z_2 of Example 2

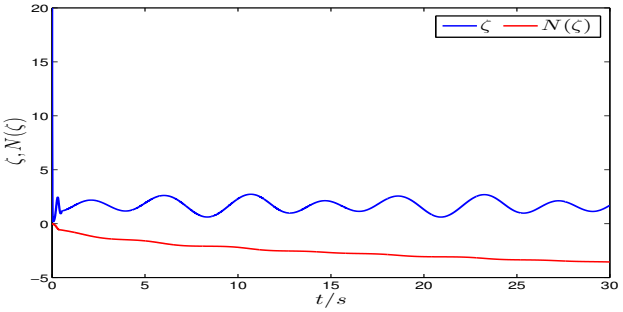

Figure 11. Nussbaum parameters of Example 2

The simulation results have clearly demonstrated that the proposed control method can be applied to the Brusselator model and achieves asymptotical tracking performance regardless the existence of the output dead-zone while the control input is constrained to the amplitude of $[-10, 10]$.

Example 3: Consider the electromechanical system described by the following equation [46]

$$\begin{cases} M\ddot{q} + B\dot{q} + N\sin(q) = I \\ L\dot{I} = V_\varepsilon - RI - K_B\dot{q} \end{cases} \tag{62}$$

where $q(t)$ represents the angular motor position, $I(t)$ is the motor armature current, and V_ε is the input control voltage. $M = \frac{J}{K_\tau} + \frac{mL_0^2}{3K_\tau} + \frac{M_0L_0^2}{K_\tau} + \frac{2M_0R_0^2}{5K_\tau}$, $N = \frac{mL_0G}{2K_\tau} + \frac{M_0L_0G}{K_\tau}$, $B = \frac{B_0}{K_\tau}$. A complete list of the parameters of the electromechanical system is given in Table I. Since the real physical system is always subject to the dead-zone output and input saturation, and the model errors inevitably exist. The dynamic model of the electromechanical system has the following state space form:

$$\begin{cases} \dot{x}_1 = x_2 \\ \dot{x}_2 = \frac{1}{M}x_3 - \frac{N}{M}\sin(x_1) - \frac{B}{M}x_2 + \frac{B}{M}\cos(x_2)\sin(x_3) \\ \dot{x}_3 = \frac{1}{L}u(v(t)) - \frac{K_B}{L} - \frac{R}{L}x_3 + \cos(x_2)\sin(x_3) \\ y = g(x_1) \end{cases} \tag{63}$$

where $x_1 = q$, $x_2 = \dot{q}$, $x_3 = I$ and $u(v(t)) = V_\varepsilon$. This system is not in a strict-feedback form. Therefore, the control methods in [46], [47] are not applicable. Since the inequalities $\frac{\partial f_2(x)}{\partial x_i} > 0$ cannot be guaranteed, the existing control methods for pure-feedback systems [40], [48] cannot be applied to control this system. With $f_2(x) = -\frac{N}{M}\sin(x_1) - \frac{B}{M}x_2 + \frac{B}{M}\cos(x_2)\sin(x_3)$, this system can be viewed as a nonstrict-feedback nonlinear systems.

Then, following the procedure presented in Section III, we design the virtual control signals (17), (18) and an adaptive neural controller (38), the tuning law (19) and two first-order filters (34). In the simulation studies, the parameters of the output dead-zone are chosen as: $m = 1, b = 0.3$. The control signal is constrained by the saturation nonlinearity characterized by the parameter $u_s = 1$. The desired trajectory is set to be $y_d = 0.5\sin(t)$. The design parameters are selected as: $k_1 = k_2 = k_3 = 5$, $\gamma = 0.5$, $k_{b1} = 0.5$, $g_m = 0.1$, $\sigma = 0.2$, $b_1 = b_2 = b_3 = 0.5$, $\tau_2 = 0.001$, $\tau_3 = 0.01$. The initial conditions are taken as: $[x_1(0), x_2(0), x_3(0)]^T = [-0.2, 1.5, 0]^T$, $\hat{\lambda}(0) = 0.5$, $[z_2(0), z_3(0)]^T = [0, 0]^T$, $\zeta(0) = 1$. Furthermore, we take the same three RBF neural networks as in Example 1 used for the approximators.

TABLE I
PARAMETERS OF THE ELECTROMECHANICAL SYSTEM OF EXAMPLE 3.

Parameter	Description	Value
J	Rotor inertia	1.625×10^{-3} kg $\cdot$ m^2
m	Link mass	0.506 kg
M_0	load mass	0.434 kg
L_0	Link length	0.305 m
R_0	Radius of the load	0.023 m
G	Gravity coefficient	9.8 N/kg
B_0	Coefficient of viscous friction	16.25×10^{-3} N $\cdot$ m/rad
K_τ	Conversion coefficient	0.9 N $\cdot$ m/A
K_B	Back-emf coefficient	0.9 N $\cdot$ m/A
L	Armature inductance	25×10^{-3} H
R	Armature resistance	5 Ω

Under the proposed adaptive dynamic surface control, it can be seen from Fig. 12 that the position of the angular motor can track the desired position in the presence of output dead-zone and input saturation. Fig. 13 shows the large

control command is generated while the saturation constraint is not violated by using the proposed control scheme. The tuning parameter adapted online and the output of the first-order filter are shown in Fig. 14 and they are bounded. To further verify the effectiveness of the proposed adaptive neural control scheme, a tracking performance comparison between the commonly used quadratic Lyapunov function (QLF)-based control algorithm and the proposed barrier Lyapunov function (BLF)-based control algorithm is implemented. Two cases given in Table II are studied, with other design conditions keeping unchanged. It is observed from Fig. 16 that the control gains affect largely the tracking control performance based on the QLF-based controller. To guarantee the tracking error constraint $|s_1(t)| \leq k_{b1} = 0.5$, the BLF-based control algorithm in this paper is used under the same condition given in Table II. The simulation result shown in Fig. 17 reveals that the effect of the control gains on the tracking performance is reduced, and the tracking error constraint is achieved and more significantly depends on the barrier parameter k_{b1} for the BLF-based control algorithm.

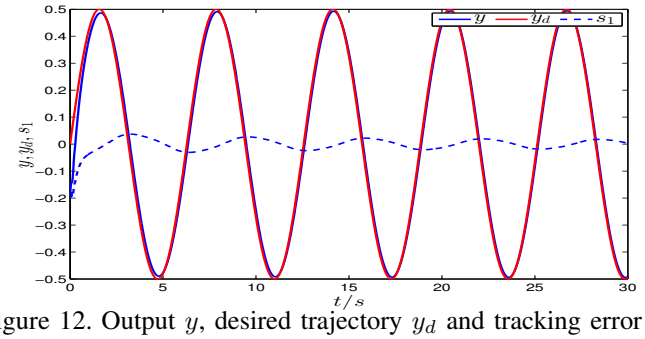

Figure 12. Output y, desired trajectory y_d and tracking error s_1 of Example 3

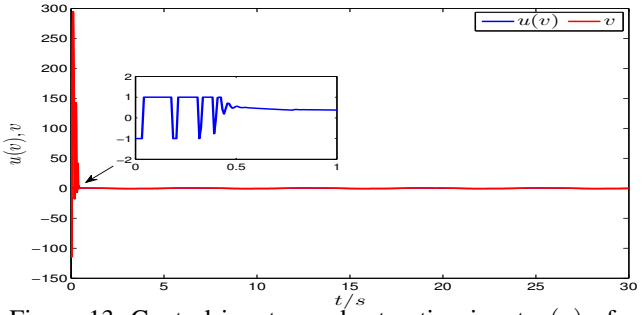

Figure 13. Control input v and saturation input $u(v)$ of Example 3

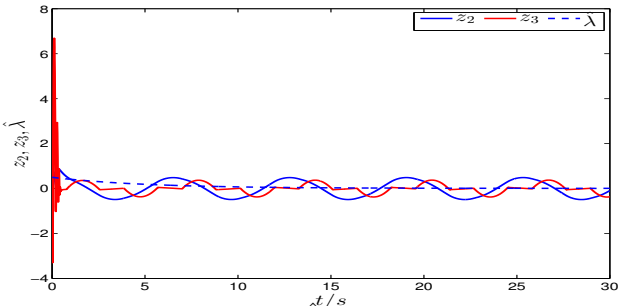

Figure 14. Adaptive parameter $\hat{\lambda}$ and filtering outputs z_2, z_3 of Example 3

TABLE II
TRACKING PERFORMANCE COMPARISON OF QLF-BASED CONTROLLER AND BLF-BASED CONTROLLER OF EXAMPLE 3.

	Case 1	Case 2
Control gains	$k_1 = k_2 = k_3 = 5$	$k_1 = k_2 = k_3 = 0.1$

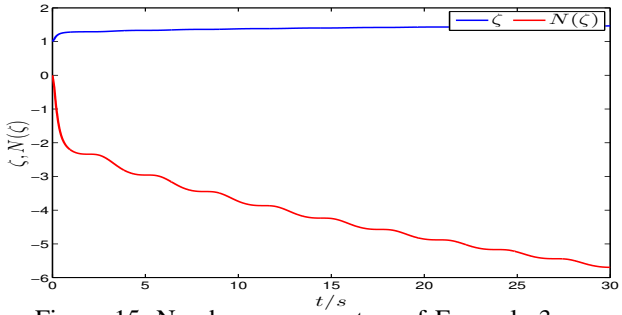

Figure 15. Nussbaum parameters of Example 3

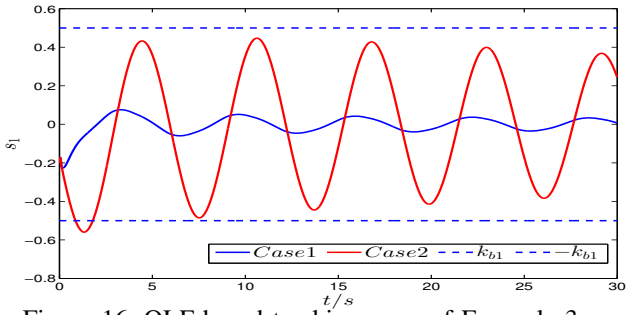

Figure 16. QLF-based tracking error of Example 3

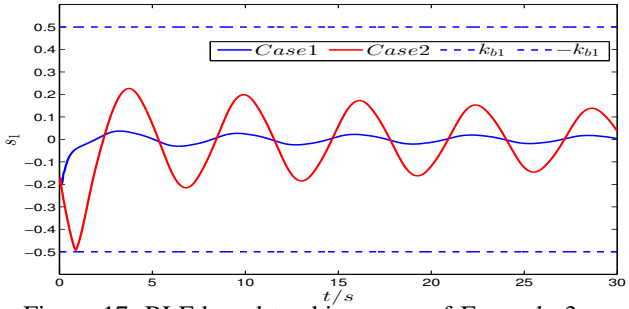

Figure 17. BLF-based tracking error of Example 3

Remark 8: It can be observed that the initial tracking performance is not desirable to some extent as shown in Fig. 4. This can be interpreted as the employment of Nussbaum function. We plot the auxiliary Nussbaum parameter ζ and the corresponding Nussbaum gain $N(\zeta)$ in Fig. 7, in which we can see that only when sufficient tracking error accumulation is achieved, the Nussbaum gain becomes negative. The tracking performance then can be improved. Figs. 8, 11, 12 and 15 illustrate the same problem in Examples 2 and 3 when applying the Nussbaum function.

V. CONCLUSIONS

In this paper, a computational efficient adaptive dynamic surface control based output-constrained tracking scheme has been developed for the stability of a class of uncertain nonstrict-feedback nonlinear systems in the presence of output

dead-zone and input saturation. Radial basis function neural networks are employed to approximate unknown continuous functions in each recursive step. By utilizing the properties of Nussbaum function, the major design difficulty arising from the unknown output dead-zone has been dealt with. The main features of the proposed control strategy are listed as follows: (1) Dynamic surface control is first employed to control nonstrict-feedback nonlinear systems. Compared with most of existing works, e.g., [3], [19]−[22], the complexity of the controller design algorithm is significantly alleviated; (2) Different from the previous control design algorithm based on the adaptive mechanism with learning parameterization, only one parameter needs to be updated online for an n-order nonlinear system, thus learning time can be drastically reduced. Meanwhile, it has been shown that all the signals of the closed-loop system are semi-global uniformly ultimately bounded via Lyapunov synthesis. Simulation results verify the effectiveness of the proposed control scheme.

The proposed control design scheme does have some conservatism when dealing with the nonstrict-feedback form. This is the issue we will look at further. In addition, several challenging problems remain to be solved, e.g., how to extend the results in this paper to stochastic nonstrict-feedback nonlinear systems, and how to design an adaptive neural output-feedback controller for system (1). These are remaining issues for further investigation.

REFERENCES

[1] Yoneyama, J. (2011). Robust guaranteed cost control of uncertain fuzzy systems under time-varying sampling. *Applied Soft Computing*, 11(1), 249-255.

[2] Joo, M. G., & Lee, J. S. (2005). A class of hierarchical fuzzy systems with constraints on the fuzzy rules. *IEEE Transactions on Fuzzy Systems*, 13(2), 194-203.

[3] Wang, H., Liu, X., Liu, K., & Karimi, H. R. (2015). Approximation-based adaptive fuzzy tracking control for a class of nonstrict-feedback stochastic nonlinear time-delay systems. *IEEE Transactions on Fuzzy Systems*, 23(5), 1746-1760.

[4] Boulkroune, A., Bouzeriba, A., & Bouden, T. (2016). Fuzzy generalized projective synchronization of incommensurate fractional-order chaotic systems. *Neurocomputing*, 173, 606-614.

[5] Bouzeriba, A., Boulkroune, A., & Bouden, T. (2016). Projective synchronization of two different fractional-order chaotic systems via adaptive fuzzy control. *Neural Computing and Applications*, 27(5), 1349-1360.

[6] Wang, T., Zhang, Y., Qiu, J., & Gao, H. (2015). Adaptive fuzzy backstepping control for a class of nonlinear systems with sampled and delayed measurements. *IEEE Transactions on Fuzzy Systems*, 23(2), 302-312.

[7] Zhou, Q., Shi, P., Liu, H., & Xu, S. (2012). Neural-network-based decentralized adaptive output-feedback control for large-scale stochastic nonlinear systems. *IEEE Transactions on Systems, Man, and Cybernetics, Part B: Cybernetics*, 42(6), 1608-1619.

[8] Liu, Z., Wang, F., Zhang, Y., & Chen, C. L. (2016). Fuzzy adaptive quantized control for a class of stochastic nonlinear uncertain systems. *IEEE Transactions on Cybernetics*, 46(2), 524-534.

[9] Chen, W., Ge, S. S., Wu, J., & Gong, M. (2015). Globally stable adaptive backstepping neural network control for uncertain strict-feedback systems with tracking accuracy known a priori. *IEEE Transactions on Neural Networks and Learning Systems*, 26(9), 1842-1854.

[10] Zhou, Q., Shi, P., Xu, S., & Li, H. (2013). Adaptive output feedback control for nonlinear time-delay systems by fuzzy approximation approach. *IEEE Transactions on Fuzzy Systems*, 21(2), 301-313.

[11] Yu, J., Shi, P., Dong, W., & Yu, H. (2015). Observer and command-filter-based adaptive fuzzy output feedback control of uncertain nonlinear systems. *IEEE Transactions on Industrial Electronics*, 62(9), 5962-5970.

[12] Liu, Y. J., Tang, L., Tong, S., & Chen, C. P. (2015). Adaptive NN controller design for a class of nonlinear MIMO discrete-time systems. *IEEE Transactions on Neural Networks and Learning Systems*, 26(5), 1007-1018.

[13] Tong, S., & Li, Y. (2013). Adaptive fuzzy output feedback control of MIMO nonlinear systems with unknown dead-zone inputs. *IEEE Transactions on Fuzzy Systems*, 21(1), 134-146.

[14] Chen, B., Liu, X., Liu, K., & Lin, C. (2013). Adaptive fuzzy tracking control of nonlinear MIMO systems with time-varying delays. *Fuzzy Sets and Systems*, 217, 1-21.

[15] Liu, Y. J., Wang, W., Tong, S. C., & Liu, Y. S. (2010). Robust adaptive tracking control for nonlinear systems based on bounds of fuzzy approximation parameters. *IEEE Transactions on Systems, Man, and Cybernetics-Part A: Systems and Humans*, 40(1), 170-184.

[16] Li, Y., & Tong, S. (2016). Hybrid adaptive fuzzy control for uncertain MIMO nonlinear systems with unknown dead-zones. *Information Sciences*, 328, 97-114.

[17] Liu, Z., Wang, F., Zhang, Y., Chen, X., & Chen, C. P. (2015). Adaptive tracking control for a class of nonlinear systems with a fuzzy dead-zone input. *IEEE Transactions on Fuzzy Systems*, 23(1), 193-204.

[18] Liu, Y. J., Li, J., Tong, S., & Chen, C. P. (2016). Neural network control-based adaptive learning design for nonlinear systems with full-state constraints. *IEEE Transactions on Neural Networks and Learning Systems*, 27(7), 1562-1571.

[19] Chen, B., Liu, X. P., Ge, S. S., & Lin, C. (2012). Adaptive fuzzy control of a class of nonlinear systems by fuzzy approximation approach. *IEEE Transactions on Fuzzy Systems*, 20(6), 1012-1021.

[20] Wang, H., Liu, X., & Liu, K. (2016). Robust adaptive neural tracking control for a class of stochastic nonlinear interconnected systems. *IEEE Transactions on Neural Networks and Learning Systems*, 27(3), 510-522.

[21] Chen, B., Zhang, H., & Lin, C. (2016). Observer-based adaptive neural network control for nonlinear systems in nonstrict-feedback form. *IEEE Transactions on Neural Networks and Learning Systems*, 27(1), 89-97.

[22] Chen, B., Liu, K., Liu, X., Shi, P., Lin, C., & Zhang, H. (2014). Approximation-based adaptive neural control design for a class of nonlinear systems. *IEEE Transactions on Cybernetics*, 44(5), 610-619.

[23] Swaroop, D., Hedrick, J. K., Yip, P. P., & Gerdes, J. C. (2000). Dynamic surface control for a class of nonlinear systems. *IEEE Transactions on Automatic Control*, 45(10), 1893-1899.

[24] Wang, D., & Huang, J. (2005). Neural network-based adaptive dynamic surface control for a class of uncertain nonlinear systems in strict-feedback form. *IEEE Transactions on Neural Networks*, 16(1), 195-202.

[25] Zhang, T. P., & Ge, S. S. (2008). Adaptive dynamic surface control of nonlinear systems with unknown dead zone in pure feedback form. *Automatica*, 44(7), 1895-1903.

[26] Yoo, S. J. (2013). Distributed consensus tracking for multiple uncertain nonlinear strict-feedback systems under a directed graph. *IEEE Transactions on Neural Networks and Learning Systems*, 24(4), 666-672.

[27] Ma, J., Zheng, Z., & Li, P. (2015). Adaptive dynamic surface control of a class of nonlinear systems with unknown direction control gains and input saturation. *IEEE Transactions on Cybernetics*, 45(4), 728-741.

[28] Han, S. I., & Lee, J. M. (2012). Adaptive fuzzy backstepping dynamic surface control for output-constrained non-smooth nonlinear dynamic system. *International Journal of Control, Automation and Systems*, 10(4), 684-696.

[29] Tong, S., Sui, S., & Li, Y. (2015). Fuzzy adaptive output feedback control of MIMO nonlinear systems with partial tracking errors constrained. *IEEE Transactions on Fuzzy Systems*, 23(4), 729-742.

[30] Zhang, T. P., & Ge, S. S. (2007). Adaptive neural control of MIMO nonlinear state time-varying delay systems with unknown dead-zones and gain signs. *Automatica*, 43(6), 1021-1033.

[31] Cui, G., Wang, Z., Zhuang, G., Li, Z., & Chu, Y. (2015). Adaptive decentralized NN control of large-scale stochastic nonlinear time-delay systems with unknown dead-zone inputs. *Neurocomputing*, 158, 194-203.

[32] Tong, S., Wang, T., & Li, Y. (2014). Fuzzy adaptive actuator failure compensation control of uncertain stochastic nonlinear systems with unmodeled dynamics. *IEEE Transactions on Fuzzy Systems*, 22(3), 563-574.

[33] Ma, H. J., & Yang, G. H. (2010). Adaptive output control of uncertain nonlinear systems with non-symmetric dead-zone input. *Automatica*, 46(2), 413-420.

[34] Zhang, Z., Xu, S., & Zhang, B. (2015). Exact tracking control of nonlinear systems with time delays and dead-zone input. *Automatica*, 52, 272-276.

[35] Zhao, X., Shi, P., Zheng, X., & Zhang, L. (2015). Adaptive tracking control for switched stochastic nonlinear systems with unknown actuator dead-zone. *Automatica*, 60, 193-200.

[36] Liu, Z., Lai, G., Zhang, Y., & Chen, C. P. (2015). Adaptive fuzzy tracking control of nonlinear time-delay systems with dead-zone output mechanism based on a novel smooth model. *IEEE Transactions on Fuzzy Systems*, 23(6), 1998-2011.

[37] Liu, Z., Lai, G., Zhang, Y., & Chen, C. L. P. (2015). Adaptive neural output feedback control of output-constrained nonlinear systems with unknown output nonlinearity. *IEEE Transactions on Neural Networks and Learning Systems*, 26(8), 1789-1802.

[38] Su, C. Y., Stepanenko, Y., Svoboda, J., & Leung, T. P. (2000). Robust adaptive control of a class of nonlinear systems with unknown backlash-like hysteresis. *IEEE Transactions on Automatic Control*, 45(12), 2427-2432.

[39] Chen, M., Tao, G., & Jiang, B. (2015). Dynamic surface control using neural networks for a class of uncertain nonlinear systems with input saturation. *IEEE Transactions on Neural Networks and Learning Systems*, 26(9), 2086-2097.

[40] Zhang, T. P., & Ge, S. S. (2008). Adaptive dynamic surface control of nonlinear systems with unknown dead zone in pure feedback form. *Automatica*, 44(7), 1895-1903.

[41] Chen, M., Ge, S. S., & Ren, B. (2011). Adaptive tracking control of uncertain MIMO nonlinear systems with input constraints. *Automatica*, 47(3), 452-465.

[42] Tee, K. P., & Ge, S. S. (2006). Control of fully actuated ocean surface vessels using a class of feedforward approximators. *IEEE Transactions on Control Systems Technology*, 14(4), 750-756.

[43] Wang, M., Chen, B., & Shi, P. (2008). Adaptive neural control for a class of perturbed strict-feedback nonlinear time-delay systems. *IEEE Transactions on Systems, Man, and Cybernetics, Part B (Cybernetics)*, 38(3), 721-730.

[44] Wang, H., Chen, B., Liu, X., Liu, K., & Lin, C. (2013). Robust adaptive fuzzy tracking control for pure-feedback stochastic nonlinear systems with input constraints. *IEEE Transactions on Cybernetics*, 43(6), 2093-2104.

[45] Ge, S. S., & Wang, C. (2002). Uncertain chaotic system control via adaptive neural design. *International Journal of Bifurcation and Chaos*, 12(5), 1097-1109.

[46] Dawson, D. M., Carroll, J. J., & Schneider, M. (1994). Integrator backstepping control of a brush DC motor turning a robotic load. *IEEE Transactions on Control Systems Technology*, 2(3), 233-244.

[47] Zhang, T., Xia, M., & Yi, Y. (2017). Adaptive neural dynamic surface control of strict-feedback nonlinear systems with full state constraints and unmodeled dynamics. *Automatica*, 81, 232-239.

[48] Liu, Y. J., & Tong, S. (2016). Barrier Lyapunov functions-based adaptive control for a class of nonlinear pure-feedback systems with full state constraints. *Automatica*, 64, 70-75.